



Published in final edited form as:

*Brain Res Bull.* 2017 January ; 128: 98–105. doi:10.1016/j.brainresbull.2016.11.008.

## Platelets are responsible for the accumulation of $\beta$ -amyloid in blood clots inside and around blood vessels in mouse brain after thrombosis

**Lilia Y. Kucheryavykh, PhD,**

Department of Biochemistry, School of Medicine, Universidad Central del Caribe, Bayamon, PR 00960-6032 (PO Box 60327), USA lilia.kucheryavykh@uccaribe.edu

**Josué Dávila-Rodríguez,**

School of Medicine, Universidad Central del Caribe, Bayamon, PR 00960-6032 (PO Box 60327), USA, jdavilero41@gmail.com

**David E. Rivera-Aponte,**

Department of Biochemistry, School of Medicine, Universidad Central del Caribe, Bayamon, PR 00960-6032 (PO Box 60327), USA, david.rivera11@upr.edu

**Lidia V. Zueva, PhD,**

Department of Physics, University of Puerto Rico Rio Piedras, San Juan, PR 00936, USA, lzueva@gmail.com

**A. Valance Washington, PhD,**

Department of Anatomy, School of Medicine, Universidad Central del Caribe, Bayamon, PR 00960-6032 (PO Box 60327), USA, and The Department of Biology, University of Puerto Rico Rio Piedras, San Juan, PR 00936, anthony.washington@upr.edu

**Priscilla Sanabria, PhD, and**

Department of Physiology, School of Medicine, Universidad Central del Caribe, Bayamon, PR 00960-6032 (PO Box 60327), USA, psanabriar@gmail.com

**Mikhail Y. Inyushin, PhD**

Department of Physiology, School of Medicine, Universidad Central del Caribe, Bayamon, PR 00960-6032 (PO Box 60327), USA

### Abstract

---

**Corresponding Author:** Mikhail Inyushin, mikhail.inyushin@uccaribe.edu.

**Competing interests:** The authors assert that there were no conflicts of interest in this research.

**Author's contributions:** All authors participated in the design of this study. AW designed and performed experiments on platelet accumulation in the ferric chloride model; LZ performed electron microscopy; DR-A and JD-R performed photothrombosis experiments and immunostaining; and MI, PS, and LK performed the imaging study. MI and LK coordinated the work and drafted the manuscript. All authors read and approved the final manuscript.

**Publisher's Disclaimer:** This is a PDF file of an unedited manuscript that has been accepted for publication. As a service to our customers we are providing this early version of the manuscript. The manuscript will undergo copyediting, typesetting, and review of the resulting proof before it is published in its final citable form. Please note that during the production process errors may be discovered which could affect the content, and all legal disclaimers that apply to the journal pertain.

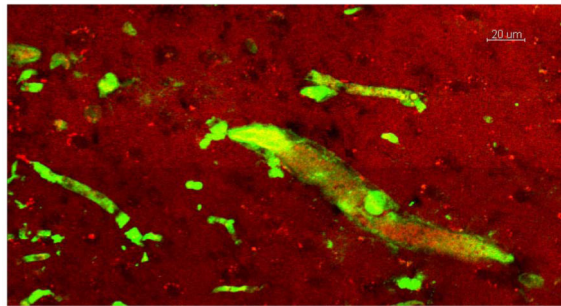
**Introduction**—Platelets contain beta-amyloid precursor protein (APP) as well as A $\beta$  peptide (A $\beta$ ) that can be released upon activation. During thrombosis, platelets are concentrated in clots and activated.

**Methods**—We used in vivo fluorescent analysis and electron microscopy in mice to determine to what degree platelets are concentrated in clots. We used immunostaining to visualize A $\beta$  after photothrombosis in mouse brains.

**Results**—Both in vivo results and electron microscopy revealed that platelets were 300–500 times more concentrated in clots than in non-clotted blood. After thrombosis in control mice, but not in thrombocytopenic animals, A $\beta$  immunofluorescence was present inside blood vessels in the visual cortex and around capillaries in the entorhinal cortex.

**Conclusion**—The increased concentration of platelets allows enhanced release of A $\beta$  during thrombosis, suggesting an additional source of A $\beta$  in the brains of Alzheimer’s patients that may arise if frequent micro-thrombosis events occur in their brains.

### Graphical abstract



### Introduction

It has long been known that amyloid precursor protein (APP) is found in megakaryocytes and subsequently in the alpha granules of platelets in relatively high concentrations ( $1.1 \pm 0.3 \mu\text{g}/10^8$  platelets) and that it is released upon platelet degranulation [1, 2, 3, 4, 5]. The total APP residing in blood plasma ( $\sim 7 \text{ ng/ml}$  [ $60 \text{ pM}$ ]) is thought to derive almost totally from platelets [1]. This blood plasma APP has been shown to be the Kunitz type protease inhibitor that affects chymotrypsin and trypsin as well as many other proteolytic proteins [2, 6]. Platelets are also the primary source of beta-amyloid peptide (A $\beta$ ) in human blood ( $\sim 90\%$ ) [7], and this secreted peptides are similar to those found in the senile plaques of Alzheimer’s patients [8]. Vessel damage is a natural cause of platelet activation and degranulation. It has been reported that circulating A $\beta$  peptide levels are elevated in patients with acute ischemic stroke [9, 10], but this condition has never been attributed to the release of A $\beta$  by platelets during clot formation.

Additionally, it has been shown that A $\beta$  peptides, monomers, and oligomers perforate cell membranes and form (at low concentrations) tetrameric channels penetrable by  $\text{K}^+$  ions. At higher concentrations, they form  $\text{Ca}^{++}$ -permeable hexameric pores [11,12,13]. An excess of  $\text{Ca}^{++}$  permeability through these pores is extremely toxic for cells, as it induces calcium

dyshomeostasis, leading to cell death [14]. Peptide antibiotics with channel-forming activity (e.g., cecropin A or nystatin) use this mechanism to kill target cells [15, 16]. Another mechanism, involving the development of A $\beta$  protofibrils that prevent pathogen adhesion to host cells, has also been proposed [17]. Recently, the activity of A $\beta$  peptide against different viruses was shown [18, 19, 20] as well as strong antibiotic activity against both Gram-negative and Gram-positive bacteria and yeast [21, 22]. These findings suggested that A $\beta$  is a hitherto unrecognized antimicrobial agent that functions as a normal component of the innate immune system [22]. We therefore hypothesize that A $\beta$  peptide released from platelets or cleaved from platelet-released APP works effectively as a natural antibiotic during clot formation following injury.

On the other hand, one of the hallmarks of Alzheimer's disease (AD) is the accumulation of A $\beta$  protein in the brain and the formation of  $\beta$ -pleated sheets and misfolded aggregations known as amyloid plaques [23, 24, 25]. Both astrocytes [26, 27] and neurons [26, 28,29] produce and release A $\beta$  to the extracellular space, which later may accumulate in plaques. This is the basis for the modern Alzheimer's concept that A $\beta$  accumulation in brain has mainly a neuronal source. Why has A $\beta$  protein of platelet origin been generally ignored? There are two possible explanations: (1) the size of platelets is significantly smaller than that of other blood cells and (2) APP and A $\beta$  are sequestered in the platelet granules and released only upon activation. Together, these explanations create the impression that the release of A $\beta$  by platelets occurs at very low concentrations. On the other hand, platelets are the second most common cell in the blood after erythrocytes (about 1 per 10 erythrocytes in mouse blood, [30]). We suggest that during thrombosis, especially in the chronic process accompanied by clot formation and an increase in platelet concentration, A $\beta$  peptide released by blood platelets or cleaved from released APP is an additional source of A $\beta$  in the brain in many cases of AD. It may have a special importance for the chronic processes accompanied by the formation of micro-clots and the increase in platelet concentration in brain blood vessels, for example during the arteriosclerosis [31,32]. Specifically, A $\beta$  protein accumulated around blood vessels forms the characteristic niche of Alzheimer's amyloid angiopathy [33, 34]. Our hypothesis is supported by the fact that activated platelets in AD patients have certain APP-processing abnormalities [35] and that in a transgenic mouse model of AD, platelets were found to be the major contributors of cerebral amyloid angiopathy [36]. Additionally, it was demonstrated that platelet-derived A $\beta$  passes through the endothelial cell layer in a blood-brain barrier model comprised of human cerebrovascular endothelial cells isolated from the brains of patients with AD [37].

In accordance with the hypothesis stated here, we used a mouse model to (1) investigate the accumulation of platelet-released A $\beta$  protein in brain blood vessels after thrombosis and (2) coordinate this process with study of the density of platelets within this zone.

We have shown that during clot formation the density of platelets in the lumen of the vessel is significantly increased (more than 300–500 times), thus allowing a massive release of A $\beta$  peptide (directly, or cleaved from released APP) at the site of clot formation. Using immunohistochemistry we have shown that A $\beta$  is concentrated in and around clotted blood vessels in the brains of animals with evoked thrombosis, while in similarly treated thrombocytopenic animals there was no specific immunostaining for A $\beta$  peptide in these

regions. While we are not studying an Alzheimer's model in this article, we suggest that this study will contribute to the current AD paradigm.

## Material and Methods

### Ethics Statement

All procedures involving rodents were conducted in accordance with the National Institutes of Health regulations concerning the use and care of experimental animals and approved by the Universidad Central del Caribe Institutional Animal Care and Use Committee. All efforts were made to minimize suffering. In all surgical experiments, animals were anesthetized with isoflurane (4% for induction and 1.75% for maintenance) using a Matrix Quantiflex VMC Anesthesia Machine for small animals (Midmark Corp., Dayton, OH). The animals were decapitated immediately after experiments, which is consistent with the recommendations of the Panel on Euthanasia of the American Veterinary Medical Association.

### Ferric chloride model

C57BL/6 female mice 8–10 weeks old were used in the experiments. Platelet-rich plasma was obtained from the heparinized whole blood of donor mice (C57BL/6 female mice of the same age), and a platelet suspension was extracted as we described previously [38]. Briefly, the blood was centrifuged at  $300 \times g$  for 10 min, and the resulting platelet-rich plasma was centrifuged once again at  $1,000 \times g$  in the presence of prostacyclin (PGI<sub>2</sub>) (0.1  $\mu\text{g}/\text{ml}$ ) for 7 min at room temperature. After two washing steps, the pelleted platelets were resuspended in modified Tyrode-Hepes buffer containing 0.35% BSA and 1 mM CaCl<sub>2</sub>. The donor platelets were then fluorescence-labeled by the addition of calcein green (5  $\mu\text{g}/\text{ml}$ ) to the suspension for 30 min. The labeled platelet suspension was then infused into recipient mice via the jugular vein under isoflurane anesthesia. The mesentery of the animals was subsequently exposed through a midline abdominal incision. Vessels with an approximate diameter of 100  $\mu\text{m}$  were used. Blood cell movement and clotting in the lumen were visualized *in vivo* with an Olympus MX21 compound microscope (Olympus, Melville NY), and fluorescence-labeled platelet accumulation was recorded with a digital camera (DC-71 digital imaging camera, Olympus Melville NY). Clot formation was generated by using a piece of filter paper (2 $\times$ 2 mm) soaked with an 8% FeCl<sub>3</sub> solution and placed over the vessel for 4 min. The filter paper was then removed, and the vessel was washed with a saline solution maintained at 37°C. Vessels were monitored for 30 min after FeCl<sub>3</sub> treatment or until cessation of blood flow (occlusion). Records were analyzed with ImageJ software (<http://rsb.info.nih.gov/ij/index.html>) using standard fluorescence integrated density (FID) measurements.

### Induction of thrombocytopenia

Induction of thrombocytopenia was achieved by intravenous injection of 0.3 ml of 5  $\mu\text{g}/\text{mL}$  anti-CD41 antibody (BD Biosciences, San Jose CA). Two hours after injection, the platelets were counted to confirm that they were reduced to less than  $100 \times 10^3/\mu\text{L}$  (in untreated control C57BL/6 animals the mean platelet count was  $1120 \pm 80 \times 10^3/\mu\text{L}$ ). If an appropriate

count was reached, the mice were subjected to photothrombosis and further histochemical and immunohistochemical analysis.

### Platelet count estimates from a blood smear examination

The traditional manual method for estimating platelet counts from Wright's-stained peripheral blood smears was used [37]. In a well-prepared smear, a semi-quantitative estimate of platelet number was made by counting the platelets visible per 100× oil immersion field in the monolayer. In general, 10 oil immersion fields were counted and the results averaged. The following formula [39] was then applied: Estimated platelet count/ $\mu\text{L}$  = average count in 10 fields  $\times$  20,000.

### Photothrombosis model

In order to induce clot formation in the mouse brain cortex, we employed a widely used method of photo-stimulated thrombosis [40,41]. We used C57BL/6 mice of both sexes, 8–10 weeks old. Briefly, prior to surgery, Rose Bengal (Sigma Chemical Co., St. Louis, MO, cat. #198250) was dissolved in a sterile saline solution (7.5 mg/ml). The mice were then anesthetized with isoflurane and restrained in a stereotaxic apparatus, followed by peritoneal injection of Rose Bengal (150  $\mu\text{g/g}$  animal weight), which was allowed to diffuse and enter the blood stream for 5 min. An incision was made along the midline from the eye level down to the neck. The skull was cleaned, and a fiber optic illuminator with a green filter (430 nm) and an intensity of 150 W was placed at the stereotaxic coordinates (bregma: caudal 3.5 mm, lateral 3.5 mm) using a 10-min exposure. The resulting thrombosis was about 3–4 mm in diameter that extended enough to include the parts in both the visual cortex and the entorhinal cortex [40]. On the next day animals were anesthetized with pentobarbital (50 mg/kg) and transcardially perfused with PBS followed by 4% paraformaldehyde (PFA). The brains were removed and postfixed in 4% PFA/PBS for 24 h at 4°C, followed by 0.15 M, 0.5 M, and 0.8 M sucrose at 4°C until fully dehydrated. The brains were then frozen-embedded in Cryo-M-Bed embedding compound (Bright Instrument, Huntingdon, England) and cut using a Vibratome UltraPro5000 cryostat (American Instrument, Haverhill, MA).

### Immunohistochemistry and confocal microscopy

Immunostaining was performed using the protocol previously established in our laboratory [43]. Frozen 25- $\mu\text{m}$  coronal sections encompassing the entire photothrombosis area were generated from each mouse brain. The sections were blocked with 5% normal goat serum/5% normal horse serum (Vector lab., Burlingame, CA) in PBS containing 0.3% Triton X-100 and 0.05% phenylhydrazine for 30 minutes and then incubated with monoclonal mouse anti-A $\beta$  antibody with very low cross-reactivity to APP (diluted 1:1000; #LS-C181965, clone MOAB-2; LifeSpan Biosciences Inc., Seattle, WA) in PBS-TAT (0.3% TritonX-100, 5% normal goat/5% normal horse serum, 1% sodium azide, 0.01% thimerosal) overnight at 4°C. The sections were incubated with the corresponding secondary antibodies (fluorescein anti-mouse IgG; Vector Lab., Burlingame, CA) overnight and visualized using an Olympus Fluoview FV1000 scanning inverted confocal microscope system equipped with a 60x/1.43 oil objective (Olympus: Melville, NY). The images were analyzed using ImageJ software (<http://imagej.nih.gov/ij>).

## Electron microscopy and platelet count

Thin (25- $\mu$ m) brain sections containing the thrombotic brain area were fixed in 2.5% glutaraldehyde with 4% PFA in 0.09 M cacodylate buffer with 0.2 mM  $\text{CaCl}_2$  for 1.5 hours at 5°C, washed with 0.09 M sodium cacodylate buffer, and postfixed in 1% osmium tetroxide ( $\text{OsO}_4$ ) with 1.5%  $\text{KFeCN}$  in the same buffer for 30 min. After treatment with 1%  $\text{OsO}_4$  for 30 min, the slices were then incubated in a 2% aqueous solution of uranyl acetate ( $\text{UO}_2(\text{CH}_3\text{OCO})_2 \cdot 2\text{H}_2\text{O}$ ) for 1 h and washed. After dehydration through a graded series of acetones, the slices were embedded in Epon/Spurr epoxy resin. Ultrathin sections of 50–60 nm were made using the Leica Ultratome and examined with a JEM100CXII electron microscope (JEOL Ltd., Japan).

Platelets and erythrocytes in clotted capillaries and small blood vessels were recognized by their shape. Their numbers were manually calculated and summarized in all photomicrographs, and the platelet/erythrocyte ratio was then calculated. Based on the literature, in non-thrombocytopenic mice the platelet/erythrocyte ratio is  $12.3 \times 10^5 / 9.23 \times 10^6 = 0.13 \approx 0.1$  [30, 44].

## Statistics

Descriptive results of continuous variables were expressed as mean  $\pm$  SD. Calculation of the correlation coefficients between the  $\text{A}\beta$  immunostaining intensity profile and the profile of the blood vessel delineated by Bengal Rose staining was used to show the degree of similarity of these profiles. A large positive correlation (at maximum, reaching 1.0) demonstrated that  $\text{A}\beta$  coincided with the vessel, and a low correlation indicated that there was little coincidence between the images; i.e.,  $\text{A}\beta$  was distributed away from the blood vessels. An unpaired two-sample t-test was performed for analysis of the difference between the visual and entorhinal cortex. We used Prism software version 5.01 (GraphPad Software) and Excel to calculate the statistics.

## Results

### 1. Platelet accumulation in clotted blood vessels is significantly higher than in normal vessels, providing the possibility of enhancing the release of $\alpha$ -granule content in the vicinity of the clot

In order to visualize clot formation in vivo we used the ferric chloride model of vascular thrombosis. Calcein-labelled platelets were infused into a recipient mouse vein, observed in blood vessels under a fluorescent microscope, and filmed for future analysis. Since the amount of fluorescence is proportional to the number of platelets, we measured the fluorescence-integrated density in the vessel lumen to reflect the density of platelets (number of cells per square unit) in the clot (see rectangle in Fig. 1). Thus, the initial platelet density can be determined before clot formation (control) at the beginning of the  $\text{FeCl}_3$  application procedure (Fig. 1A). In the control, the movement of platelets was unrestricted (Supplemental File S1), and the fluorescent cells moved rapidly with the blood. Two to three minutes after initiation of clot formation, platelets were accumulating inside the blood vessel clot with increasing density (Fig. 1B). A video shows that the fluorescent cells in this area were immobilized, and blood flow was stopped (Supplemental File S1). A summary of the



fluorescence density measurements from 10 separate experiments is shown in Fig. 1. Three minutes after initiation of coagulation, the mean density of platelets in the clot was 536 times greater than in an unclotted vessel (Fig. 1C).

## 2. Platelets are the most numerous cell type in the blood clot

Electron microscopy of clotted brain blood vessels revealed that platelets are the main cell type in clotted blood inside small capillaries ( $< 9 \mu\text{m}$  in diameter), in which the platelet/erythrocyte ratio, estimated from photomicrographs, was  $31 \pm 1.2$  ( $n=14$ , Fig. 2A). In larger vessels, clots contained more erythrocytes, but platelets were unevenly distributed inside the vessel, occupying mostly the space near the endothelial wall (Fig. 2B). These platelets were mostly touching one another and the endothelial walls, conglomerating near the vessel wall and reaching a platelet/erythrocyte ratio similar to clots in small blood vessels (Fig. 2B). According to these results and taking into account that the normal ratio of platelets to erythrocytes in mouse blood is  $\sim 0.1$ , we conclude that in the capillary clot the platelet count was significantly higher:  $31/0.1 = 310$  times.

## 3. Photothrombosis induced in the visual cortex causes accumulation of A $\beta$ peptide inside blood vessels

Immunostaining for A $\beta$  peptide after photo-induced thrombosis in the visual cortex in C57BL/6J mice revealed the accumulation of A $\beta$  peptides, mainly in blood clots formed inside vessels (Fig. 3). Formation of blood clots was visualized by the accumulation of red fluorescence in red blood cells in clots and in blood vessel walls, caused by preferential accumulation of the fluorescent Rose Bengal dye [45] used for photothrombosis, as illustrated in Fig. 3A. Similarly, A $\beta$  immunofluorescence was detected mainly inside small capillaries, as illustrated in Fig. 3A, B.

Thrombocytopenic animals subjected to photo-induced thrombosis were used to determine whether platelets are the primary source of the A $\beta$  protein visualized in blood clots. Temporary thrombocytopenia was induced in C57BL/6 mice by single injection of antiplatelet anti-CD41 antibody, with a resulting depletion of blood platelets to less than 10% of the normal level. Two figures exemplify this process: the immunostaining of A $\beta$  in control (Fig. 4A) and thrombocytopenic (Fig. 4B) animals. Control animals' capillaries were clearly marked by A $\beta$ -peptide-related fluorescence, but there was no evidence of any A $\beta$ -specific staining in animals with depleted platelets. This observation implicates platelets as not only the main player in the process of clot formation but also as a source of A $\beta$  released into blood vessels during this process.

## 4. Photothrombosis induced in the mouse entorhinal cortex causes an accumulation of A $\beta$ peptide outside the blood vessels

There was a noticeable difference in the distribution of A $\beta$  peptide immunofluorescence in blood capillaries of the visual and entorhinal cortex of mouse brains. While A $\beta$  peptide-related fluorescence was mainly associated with the capillary lumen in the visual cortex (Fig. 3A, B and Fig. 4A), in the entorhinal cortex immunofluorescence was also detected a short distance from ( $< 10 \mu\text{m}$ ) but on the outside of the blood vessels (Fig. 5A). Using ImageJ software (<https://imagej.nih.gov/ij/>) we analyzed transverse optical cuts of the

vessels in both the visual and entorhinal cortex and made plots across the diameter (Dm) of the vessel, using two channels (green for the A $\beta$  peptide-related fluorescence and red for Rose Bengal fluorescence, Fig. 5B, C). In the entorhinal cortex, a plot of A $\beta$  fluorescence shows the distribution of A $\beta$  protein around the red fluorescence corresponding to erythrocytes in the capillary lumen (Fig. 5B). By contrast, in the visual cortex the A $\beta$  immunofluorescence was concentrated in the lumen and mainly coincided with the red fluorescence of erythrocytes and the blood vessel wall (Fig. 5C). Comparing the correlation between the green and the red channels ( $0.78 \pm 0.15$  in the visual cortex, a relatively high correlation;  $0.07 \pm 0.17$  in the entorhinal cortex, a very low correlation; N=4), it was found that, in contrast to the visual cortex (N=4;  $t = 0.0098$ ;  $P < 0.01$ ), where the A $\beta$  fluorescence was mostly observed inside the blood vessels, A $\beta$  in the entorhinal cortex was distributed away from the blood vessels in the surrounding tissue.

Furthermore, we did not find any specific immunostaining of A $\beta$  peptide in mice with induced thrombocytopenia. These results show a difference in the distribution of A $\beta$  peptide released by platelets (or cleaved from APP released by platelets) in different areas of the cortex.

## Discussion

In this study we demonstrated that platelets specifically accumulate in the affected part of a vessel during the clot formation process. Platelet adhesion to the subendothelium and the vessel walls following vascular injury is a well-known event, and it was previously observed that platelet adhesion occurs before the clot is formed and blood flow is stopped [46]. We suggested that the concentration of platelets in the clot offers the possibility of massive release of  $\alpha$ -granule contents, including A $\beta$  and APP [1, 7]. Thus the purpose of this study was to determine to what extent platelets are concentrated in the clot. Using the ferric chloride model of clot formation and fluorescent platelet recording we discovered that the density of platelets in blood vessels in the area of the thrombosis was at a concentration 500 times that of non-thrombotic vessels (Fig. 1, Supplementary File S1). Because of the limited depth of field of the microscope, these measurements do not take into account the three-dimensionality of the clot. Therefore, the actual concentration of platelets in the clotted area is expected to be even higher.

For a direct count and more precise calculations of the concentration of platelets and erythrocytes in clotted brain blood vessels, we used electron photomicrographs (Fig. 2). In this way we found 300 times more platelets in the clot compared with non-clotted blood. It is known that during clot formation and platelet activation the content of the  $\alpha$ -granules is released [47]. Platelet  $\alpha$ -granules are specialized storage vesicles containing A $\beta$  and have been shown to release large amounts of A $\beta$  and APP upon activation. The accumulation of platelets in the clot therefore provides the possibility of concentrated release of A $\beta$  and APP. While the standard concentration of A $\beta$  and APP in the blood is about 7 ng/ml and is almost totally derived from de-granulated platelets [1], after an increase in platelet concentration of 300 to 500 times, the concentration of A $\beta$  and APP can be estimated to reach levels as high as 2–3.5  $\mu$ g/ml inside the clot.



Our results demonstrate that, following thrombosis in mouse brain cortex, A $\beta$  peptides are detected in and around blood vessels in control animals but not in thrombocytopenic animals (Figs. 3–5). These results implicate platelets as the most likely source of A $\beta$  peptides in blood and brain tissues. The other sources of A $\beta$  peptides in brain tissue were previously reported: both astrocytes [27] and neurons [28, 29] produce and release A $\beta$  to the extracellular space. However, the role of platelets in the release and accumulation of A $\beta$  in brain tissue is generally underestimated. Blood platelets can be an important additional source of A $\beta$  in the brain, especially in A $\beta$  accumulation around blood vessels, since A $\beta$  is directly released by platelets [2, 7] or cleaved from platelet-released APP. APP, in turn, is cleaved immediately after release by APP-cleaving enzyme 1 (BACE1), located on the platelet membrane [48, 49], or by the endothelial cells of brain blood vessels [50]. MOAB-2 [NBP2-13075] (mouse IgG2b), the anti-A $\beta$  antibody used in this study, was extensively examined previously and was found to be a pan-specific, high-titer antibody to A $\beta$  residues 1–4, reacting with unaggregated, oligomeric, and fibrillar forms of A $\beta$ 42 and unaggregated A $\beta$ 40 as well as with aggregated amyloid in plaques [51,52]. MOAB-2 anti-A $\beta$  antibody did not detect APP or its derivatives and did not colocalize with antibodies to either N- or C-terminal APP [49].

Our results revealed a difference in A $\beta$  accumulation in and around blood vessels in dissimilar cortical areas affected by thrombosis (Fig. 5). While the capillary lumen was the main location of A $\beta$ -related fluorescence in the visual cortex (Fig. 3A, B and Fig. 4A), in the entorhinal cortex the immunofluorescence was distributed within a short distance (< 10  $\mu$ m) outside of the blood vessels (Fig. 5A). These results match well with medical observations indicating that the entorhinal cortex is the area of the cortex primarily affected by AD [53,54]. We speculate that this area of the cortex might have a related variation in certain biochemical factors, for example in the A $\beta$  transporters that are responsible for maintaining both the influx and efflux of A $\beta$  across the blood–brain barrier (BBB).

As has been shown by Shayo et al. [55], A $\beta$  protein can pass through the BBB by the mechanism of binding to apolipoproteins. More recently it was proposed that the receptor for advanced glycation end products (RAGE) is involved in the influx transport of A $\beta$  [56]. The low-density lipoprotein receptor-related protein 1 (LRP1) [57] as well as P-glycoprotein a (also known as ABCB1) and BCRP (also known as ABCG2) [58] were shown to be involved in A $\beta$  efflux from the brain.

Generally, there must be a balance between A $\beta$  accumulated in the brain from different sources and the clearance of accumulated amyloid, suggesting an interchange between the periphery and the brain through the BBB, in which the blood serves as a peripheral sink for the peptide. This peripheral sink hypothesis is based on the influx–efflux transport across the brain vessel walls into the blood stream. It was shown in recent work that continued inhibition of peripheral BACE1 affects the brain levels of A $\beta$  much less than the peripheral levels [59]. In addition, degrading A $\beta$  only peripherally with neprilysin does not affect the central levels of A $\beta$  [60]. These findings indicate that A $\beta$  does not directly diffuse back from the brain through the BBB. This hypothesis may be corroborated by the recent discovery of the glymphatic system, suggesting that A $\beta$  can be removed from brain tissue without crossing back to the blood using perivascular clearance pathways [61,62]. These

findings suggest that transport from blood to the brain is still viable, and we speculate that A $\beta$  peptides released by platelets or cleaved from released APP add to the cerebral amyloid burden. Platelets also participate in the development of arteriosclerosis and subsequent vascular remodeling and may be a source of A $\beta$  found in sclerotic plaques [63,64]. It was previously discovered that in AD transgenic mice, platelets accumulate at amyloid deposits of cerebral vessels and induce thrombosis, confirming that platelets are major contributors to cerebral amyloid angiopathy [36].

Another mechanism of A $\beta$  peptide removal from blood clots was reported recently: it was shown that plasmin (a fibrinolytic enzyme that dissolves clots), degrades A $\beta$  [65,66]. This mechanism of A $\beta$  removal from clots is found to be reduced in AD patients [67].

We want to stress that this study was focused on the evaluation in brain blood vessels of A $\beta$  peptide, which is a fragment of the precursor molecule APP resulting from specific cleavage and not the entire APP molecule. It has been shown that not just the A $\beta$  peptide but certain other APP fragments perforate cell plasma membranes [66] and acquire antimicrobial and antifungal effects. Additionally, APP released from platelets contains a Kunitz-type protease inhibitor, which effectively inhibits chymotrypsin, trypsin, and other proteolytic enzymes [2, 6, 67] and promotes the activation of coagulation factor XII [69,70]. Therefore, platelet-released APP is likely to play an important role in the hemostasis and temporal stability of the thrombus [69].

Our results suggest that A $\beta$  release from platelets is a naturally occurring event during the normal blood clotting process in the brain and other tissues. It was suggested that platelets are an important part of an ancient defense system, interacting with bacterial pathogens through a wide array of cellular and molecular mechanisms [71,72], and platelets and oligomeric A $\beta$  are efficient antibacterial weapons [22]. Why this normal release of A $\beta$  leads to uncontrollable accumulation of amyloid deposits in the brain is still an enigma to be resolved.

## Conclusions

- A $\beta$  peptides accumulate inside and around blood vessels in mice in the visual and entorhinal cortex following induced thrombosis.
- The high concentration of platelets inside clotted blood vessels allows the massive release of A $\beta$ .

## Supplementary Material

Refer to Web version on PubMed Central for supplementary material.

## Acknowledgments

The authors wish to thank the personnel of the Gemology Department at Dr. Ramon Ruiz Arnau University Hospital (Puerto Rico) for their help with Wright staining for platelet counting.

This research was supported by NIH/ NIMHD 5SC2GM102040 Grant to L.K., NIH/NINDS SNRP Grant 1U54 N 5083924 to L. Z., NIH/ NIMHD Grant 5G12MD007583 to P.S. and to M.I., and NIH/ NIMHD Grant

1SC2GM111149 to M.I. , R25GM110513 for D. R.-A., NIH Grant R01HL90933 to A. V. W. Funding sources had no role in study design; collection, analysis and interpretation of data or the decision to submit this article.

## Abbreviations

<b>A<math>\beta</math></b>	amyloid beta
<b>APP</b>	amyloid precursor protein
<b>BBB</b>	blood–brain barrier
<b>AD</b>	Alzheimer's disease

## Reference

1. Bush AI, Martins RN, Rumble B, Moir R, Fuller S, Milward E, Currie J, David Amesn, Andreas Weidemannll, Fischer R, Multhaup G, Beyreuther K, Masters CL. The amyloid precursor protein of Alzheimer's disease is released by human platelets. *J Biol Chem.* 1990; 265:15977–15983. [PubMed: 2118534]
2. Van Nostrand WE, Schmaier AH, Farrow JS, Cunningham DD. Protease nexin-II (amyloid beta-protein precursor): a platelet alpha-granule protein. *Science.* May 11; 1990 248(4956):745–8. [PubMed: 2110384]
3. Rosenberg RN, Baskin F, Fosmire JA, Risser R, Adams P, Svetlik D, Honig LS, Cullum CM, Weiner MF. Altered amyloid protein processing in platelets of patients with Alzheimer disease. *Arch Neurol.* 1997; 54:139–144. [PubMed: 9041854]
4. Baskin F, Rosenberg RN, Iyer L,L, Hynan L, Cullum CM. Platelet APP isoform ratios correlate with declining cognition in AD. *Neurology.* 2000; 54:1907–1909. [PubMed: 10822427]
5. Padovani A, Pastorino L, Borroni B, Colciaghi F, Rozzini L, Monastero R, Perez J, Pettenati C, Mussi M, Parrinello G, Cottini E, Lenzi GL, Trabucchi M, Cattabeni F, Di Luca M. Amyloid precursor protein in platelets:a peripheral marker for the diagnosis of sporadic AD. *Neurology.* 2001; 57:2243–2248. [PubMed: 11756604]
6. Van Nostrand WE, Schmaier AH, Farrow JS, Cines DB, Cunningham DD. Protease nexin- 2/ amyloid beta-protein precursor in blood is a platelet-specific protein. *Biochem Biophys Res Commun.* Feb 28; 1991 175(1):15–21. [PubMed: 1900151]
7. Chen M, Inestrosa CC, Ross GS, Fernandez HL. Platelets are the primary source of amyloid P-peptide in human blood. *Biochem Biophys Res Commnun.* 1995; 213:96–103.
8. Scheuner D, Eckman C, Jensen M, Song X, Citron M, Suzuki N, Bird TD, Hardy J, Hutton M, Kukull W, Larson E, Levy-Lahad E, Viitanen M, Peskind E, Poorkaj P, Schellenberg G, Tanzi R, Wasco W, Lannfelt L, Selkoe D, Younkin S. Secreted amyloid P-protein similar to that in the senile plaques of Alzheimer's disease is increased in vivo by the presenilin 1 and 2 and APP mutations linked to familial Alzheimer's disease. *Nat Med.* 1996; 2:864–870. [PubMed: 8705854]
9. Lee PH, Bang OY, Hwang EM, Lee JS, Joo US, Mook-Jung I, Huh K. Circulating beta amyloid protein is elevated in patients with acute ischemic stroke. *J. Neur. Transm.* 2005; 112(Number 10): 1371–1379.
10. Aho L, Jolkkonen J, Alafuzoff I.  $\beta$ -Amyloid Aggregation in Human Brains With Cerebrovascular Lesions. *Stroke.* 2006; 37:2940–2945. [PubMed: 17095738]
11. Kawahara M, Arispe N, Kuroda Y, Rojas E. Alzheimer's disease amyloid beta-protein forms Zn(2+)-sensitive, cation-selective channels across excised membrane patches from hypothalamic neurons. *Biophys J.* Jul; 1997 73(1):67–75. [PubMed: 9199772]
12. Lin H, Bhatia R, Lal R. Amyloid beta protein forms ion channels: implications for Alzheimer's disease pathophysiology. *FASEB J.* Nov; 2001 15(13):2433–44. [PubMed: 11689468]
13. Lal R, Lin H, Quist AP. Amyloid beta ion channel: 3D structure and relevance to amyloid channel paradigm. *Biochim Biophys Acta.* Aug; 2007 1768(8):1966–75. Epub 2007 May 3. [PubMed: 17553456]

14. Kawahara M. Neurotoxicity of  $\beta$ -amyloid protein: oligomerization, channel formation, and calcium dyshomeostasis. *Curr Pharm Des.* 2010; 16(25):2779–89. [PubMed: 20698821]
15. Harder J, Bartels J, Christophers E, Schröder J-M. A peptide antibiotic from human skin. *Nature.* 1997; 387:861. [PubMed: 9202117]
16. Hancock, REW.; Chapple, DS. *Antimicrob Agents and Chemotherapy.* Jun. 1999 Peptide Antibiotics; p. 1317-132.
17. Kumar DK, Choi SH, Washicosky KJ, Eimer WA, Tucker S, Ghofrani J, Lefkowitz A, McColl G, Goldstein LE, Tanzi RE, Moir RD. Amyloid- $\beta$  peptide protects against microbial infection in mouse and worm models of Alzheimer's disease. *Sci Transl Med.* May 25.2016 8(340): 340ra72.doi: 10.1126/scitranslmed.aaf1059
18. White MR, Kandel R, Tripathi S, et al. Alzheimer's associated  $\beta$ -Amyloid protein inhibits influenza a virus and modulates viral interactions with phagocytes. *PLoS One.* 2014; 9(7):1–9. DOI: 10.1371/journal.pone.0101364
19. Bourgade K, Garneau H, Giroux G, et al. Amyloid peptides display protective activity against the human Alzheimer's disease-associated herpes simplex virus-1. *Biogerontology.* 2014; 16(1):85–98. DOI: 10.1007/s10522-014-9538-8 [PubMed: 25376108]
20. Lukiw WJ, Cui JG, Yuan LY, et al. Acyclovir or A $\beta$ 42 peptides attenuate HSV-1-induced miRNA-146a levels in human primary brain cells. *Neuroreport.* 2010; 21(14):922–927. DOI: 10.1097/WNR.0b013e32833da51a [PubMed: 20683212]
21. Papareddy P, Mörgelin M, Walse B, Schmidtchen A, Malmsten M. Antimicrobial activity of peptides derived from human  $\beta$ -amyloid precursor protein. *J Pept Sci.* 2012; 18(3):183–191. DOI: 10.1002/psc.1439 [PubMed: 22249992]
22. Soscia SJ, Kirby JE, Washicosky KJ, Tucker SM, Ingelsson M, Hyman B, Burton MA, Goldstein LE, Duong S, Tanzi RE, Moir RD. Bush, Ashley The Alzheimer's Disease-Associated Amyloid  $\beta$ -Protein Is an Antimicrobial Peptide. *PLoS ONE.* 2010; 5(3):e9505. [PubMed: 20209079]
23. Kirschner DA, Abraham C, Selkoe DJ. X-ray diffraction from intraneuronal paired helical filaments and extraneuronal amyloid fibers in Alzheimer disease indicates cross- $\beta$  conformation. *Proceedings of the National Academy of Sciences of the United States of America.* 1986; 83(no. 2):503–507. [PubMed: 3455785]
24. Selkoe DJ. Alzheimer's disease: genes, proteins, and therapy. *Physiol Rev.* 2001; 81:741–766. [PubMed: 11274343]
25. LaFerla FM, Green KN, Oddo S: Intracellular amyloid- $\beta$  in Alzheimer's disease. *Nat Rev Neurosci.* 2007; 8:499–508. [PubMed: 17551515]
26. Busciglio J, Gabuzda DH, Matsudaira P, Yankner BA. Generation of b-amyloid in the secretory pathway in neuronal and nonneuronal cells. *Proc. Natl. Acad. Sci. U.S.A.* 1993; 90:2092–2096. [PubMed: 8446635]
27. Shepherd CE, Bowes S, Parkinson D, Cambray-Deakin M, Pearson RCA. Expression of amyloid precursor protein in human astrocytes in vitro: isoform-specific increases following heat shock. *Neuroscience, V99.* 2000; 2:317–325.
28. Simons M, et al. Amyloidogenic processing of the human amyloid precursor protein in primary cultures of rat hippocampal neurons. *J. Neurosci.* 1996; 16:899–908.
29. Hook V, Toneff T, Bogyo M, Greenbaum D, Medzihradzky KF, Neveu J, Lane W, Hook G, Reisine T. Inhibition of cathepsin B reduces  $\beta$ -amyloid production in regulated secretory vesicles of neuronal chromaffin cells: evidence for cathepsin B as a candidate  $\beta$ -secretase of Alzheimer's disease. *Biological Chemistry.* 2005; 386(9):931–940. [PubMed: 16164418]
30. Barrios M, Rodríguez-Acosta A, Gil A, Salazar AM, Taylor P, Sánchez EE, Arocha-Piñango CL, Guerrero B. Comparative hemostatic parameters in BALB/c, C57BL/6 and C3H/He mice. *Thromb Res.* Jul; 2009 124(3):338–43. [PubMed: 19101712]
31. Holvoet P, Collen D. Thrombosis and atherosclerosis. *Curr Opin Lipidol.* Oct; 1997 8(5):320–8. [PubMed: 9335957]
32. Badimon L, Vilahur G. Thrombosis formation on atherosclerotic lesions and plaque rupture. *J Intern Med.* Dec; 2014 276(6):618–32. DOI: 10.1111/joim.12296 [PubMed: 25156650]
33. Vinters HV. Cerebral amyloid angiopathy: a critical review. *Stroke.* 1987; 18:311–324. [PubMed: 3551211]

34. Weller RO, Nicoll JA. Cerebral amyloid angiopathy: pathogenesis and effects on the ageing and Alzheimer brain. *Neurol Res. Sep; 2003 25(6):611–6.* [PubMed: 14503015]
35. Davies TA, Long HJ, Sgro K, Rathbun WH, McMenamin ME, Seetoo K, Tibbles H, Billingslea AM, Fine RE, Fishman JB, Levesque CA, Smith SJ, Wells JM, Simons ER. Activated Alzheimer disease platelets retain more beta amyloid precursor protein. *Neurobiol Aging. Mar-Apr;1997 18(2):147–53.* [PubMed: 9258891]
36. Gowert NS, Donner L, Chatterjee M, Eisele YS, Towhid ST, Münzer P, Walker B, Ogorek I, Borst O, Grandoch M, Schaller M, Fischer JW, Gawaz M, Weggen S, Lang F, Jucker M, Elvers M. Blood Platelets in the Progression of Alzheimer's Disease. *PLoS ONE. 2014; 9(2):e90523.* [PubMed: 24587388]
37. Davies TA, Long HJ, Eisenhauer PB, Hasteley R, Cribbs DH, Fine RE, Simons ER. Beta amyloid fragments derived from activated platelets deposit in cerebrovascular endothelium: usage of a novel blood brain barrier endothelial cell model system. *Amyloid. Sep; 2000 7(3):153–65.* [PubMed: 11019856]
38. Washington VA, Gibot S, Acevedo I, Gattis J, Quigley L, Feltz R, De La Mota A, Schubert RL, Gomez-Rodriguez J, Cheng J, Dutra A, Pak E, Chertov O, Rivera L, Morales J, Lubkowski J, Hunter R,L, Schwartzberg PL, Daniel W, McVicar DW. TREM-like transcript-1 protects against inflammation-associated hemorrhage by facilitating platelet aggregation in mice and humans. *J Clin Invest. Jun 1; 2009 119(6):1489–1501.* DOI: 10.1172/JCI36175 [PubMed: 19436112]
39. Malok M, Titchener EH, Bridgers C, Lee BY, Bamberg R. Comparison of two platelet count estimation methodologies for peripheral blood smears. *Clin Lab Sci. 2007 Summer;20(3):154–60.* [PubMed: 17691671] Schnell MA, Hardy C, Hawley M, Propert KJ, Wilson JM. Effect of blood collection technique in mice on clinical pathology parameters. *Hum Gene Ther. Jan 1; 2002 13(1): 155–61.* [PubMed: 11779419]
40. Watson BD, Dietrich WD, Busto R, Wachtel MS, Ginsberg MD. Induction of reproducible brain infarction by photochemically initiated thrombosis. *Ann. Neurol. 1985; 17:497–504.* [PubMed: 4004172]
41. Labatgest V, Tomasi S. Photothrombotic ischemia: a minimally invasive and reproducible photochemical cortical lesion model for mouse stroke studies. *J Vis Exp. Jun 9.2013 (76)*
42. Paxinos, G.; Franklin, KBJ. *The Mouse Brain in Stereotaxic Coordinates.* Fourth Edition. Academic Press; 2012. p. 1-555.
43. Kucheryavykh L, Kucheryavykh Y, Rolón-Reyes K, Skatchkov S, Eaton M, Cubano L, Inyushin M. Visualization of implanted GL261 glioma cells in mouse brain using fluorescent 4-(4-(dimethylamino)-styryl)-N-methylpyridinium iodide (ASP+). *Biotechniques. Oct.2012 :1–4.* 2012. 0(0).
44. Schnell MA, Hardy C, Hawley M, Propert KJ, Wilson JM. Effect of blood collection technique in mice on clinical pathology parameters. *Hum Gene Ther. Jan 1; 2002 13(1):155–61.* [PubMed: 11779419]
45. Neckers DC, Rose Bengal. *J.Photochem. Photobiol. A.* 1989; 47(1):1–29.
46. Rumbaut, RE.; Thiagarajan, P. *Platelet-Vessel Wall Interactions in Hemostasis and Thrombosis (the book).* Morgan & Claypool Life Sciences; San Rafael (CA): 2010.
47. White JG. Exocytosis of secretory organelles from blood platelets incubated with cationic polypeptides. *Am J Pathol. Oct; 1972 69(1):41–54.* [PubMed: 5080705]
48. Evin G, Zhu A, Holsinger RM, Masters CL, Li QX. Proteolytic processing of the Alzheimer's disease amyloid precursor protein in brain and platelets. *J Neurosci Res. Nov 1; 2003 74(3):386–92.* [PubMed: 14598315]
49. Johnston JA, Liu WW, Todd SA, Coulson DT, Murphy S, Irvine GB, Passmore AP. Expression and activity of beta-site amyloid precursor protein cleaving enzyme in Alzheimer's disease. *Biochem Soc Trans. Nov; 2005 33(Pt 5):1096–100.* [PubMed: 16246054]
50. Davies TA, Billingslea AM, Long HJ, Tibbles H, Wells JM, Eisenhauer PB, Smith SJ, Cribbs DH, Fine RE, Simons ER. Brain endothelial cell enzymes cleave platelet-retained amyloid precursor protein. *J Lab Clin Med. Oct; 1998 132(4):341–50.* [PubMed: 9794706]
51. Youmans KL, Tai LM, Kanekiyo T, Stine WB Jr, Michon SC, Nwabuisi-Heath E, Manelli AM, Fu Y, Riordan S, Eimer WA, Binder L, Bu G, Yu C, Hartley DM, LaDu MJ. Intraneuronal A $\beta$

- detection in 5xFAD mice by a new A $\beta$ -specific antibody. *Mol Neurodegener.* Mar 16.2012 7:8. [PubMed: 22423893]
52. Collins JM, King AE, Woodhouse A, Kirkcaldie MT, Vickers JC. The effect of focal brain injury on beta-amyloid plaque deposition, inflammation and synapses in the APP/PS1 mouse model of Alzheimer's disease. *Exp Neurol.* May.2015 267:219–29. DOI: 10.1016/j.expneurol.2015.02.034 [PubMed: 25747037]
  53. Braak H, Braak E. Neuropathological staging of Alzheimer-related changes. *Acta Neuropathol.* 1991; 82(4):239–59. [PubMed: 1759558]
  54. Yeh CY, Vadhvana B, Verkhatsky A, Rodríguez JJ. Early astrocytic atrophy in the entorhinal cortex of a triple transgenic animal model of Alzheimer's disease. *ASN Neuro.* Dec 19; 2011 3(5): 271–9. [PubMed: 22103264]
  55. Shayo M, McLay RN, Kastin AJ, Banks WA. The putative blood-brain barrier transporter for the beta-amyloid binding protein apolipoprotein j is saturated at physiological concentrations. *Life Sci.* 1997; 60(7):PL115–8. [PubMed: 9042383]
  56. Deane R, Du Yan S, Subramanian RK, LaRue B, Jovanovic S, Hogg E, Welch D, Manness L, Lin C, Yu J, Zhu H, Ghiso J, Frangione B, Stern A, Schmidt AM, Armstrong DL, Arnold B, Liliensiek B, Nawroth P, Hofman F, Kindy M, Stern D, Zlokovic B. RAGE mediates amyloid-beta peptide transport across the blood-brain barrier and accumulation in brain. *Nat Med.* Jul; 2003 9(7):907–13. [PubMed: 12808450]
  57. Deane R, Bell RD, Sagare A, Zlokovic BV. Clearance of amyloid-beta peptide across the blood-brain barrier: implication for therapies in Alzheimer's disease. *CNS Neurol Disord Drug Targets.* Mar; 2009 8(1):16–30. [PubMed: 19275634]
  58. Zhang W, Xiong H, Callaghan D, Liu H, Jones A, Pei K, Fatehi D, Brunette E, Stanimirovic D. Blood-brain barrier transport of amyloid beta peptides in efflux pump knock-out animals evaluated by in vivo optical imaging. *Fluids Barriers CNS.* Feb 25.2013 10(1):13.doi: 10.1186/2045-8118-10-13 [PubMed: 23432917]
  59. Georgievska B, Gustavsson S, Lundkvist J, Neelissen J, Eketjäll S, Ramberg V, Bueters T, Agerman K, Juréus A, Svensson S, Berg S, Fälting J, Lendahl U. Revisiting the peripheral sink hypothesis: inhibiting BACE1 activity in the periphery does not alter  $\beta$ -amyloid levels in the CNS. *J Neurochem.* Feb; 2015 132(4):477–86. [PubMed: 25156639]
  60. Henderson SJ, Andersson C, Narwal R, Janson J, Goldschmidt TJ, Appelkvist P, Bogstedt A, Steffen AC, Haupts U, Tebbe J, Freskgård PO, Jermutus L, Burrell M, Fowler SB, Webster CI. Sustained peripheral depletion of amyloid- $\beta$  with a novel form of neprilysin does not affect central levels of amyloid- $\beta$ . *Brain.* Feb; 2014 137(Pt 2):553–64. [PubMed: 24259408]
  61. Weller RO, Subash M, Preston SD, Mazanti I, Carare RO. Perivascular drainage of amyloid-beta peptides from the brain and its failure in cerebral amyloid angiopathy and Alzheimer's disease. *Brain Pathol.* 2008; 18(2):253–266. [PubMed: 18363936]
  62. Louveau A, Smirnov I, Keyes TJ, Eccles J, Rouhani SJ, Peske JD, Derecki NC, Castle D, Mandell JW, Lee KS, Harris TH, Kipnis J. Structural and functional features of central nervous system lymphatic vessels. *Nature.* Jul 16; 2015 523(7560):337–41. [PubMed: 26030524]
  63. Tedgui A, Mallat Z. Platelets in Atherosclerosis, A New Role for  $\beta$ -Amyloid Peptide Beyond Alzheimer's Disease. *Circulation Research.* 2002; 90:1145–1146. [PubMed: 12065314]
  64. King SM, McNamee RA, Houg AK, Patel R, Brands M, Reed GL. Platelet dense-granule secretion plays a critical role in thrombosis and subsequent vascular remodeling in atherosclerotic mice. *Circulation.* Sep 1; 2009 120(9):785–91. [PubMed: 19687360]
  65. Tucker HM, Kihiko-Ehmann M, Wright S, Rydel RE, Estus S. Tissue plasminogen activator requires plasminogen to modulate amyloid-beta neurotoxicity and deposition. *J Neurochem.* 2000; 75:2172–2177. [PubMed: 11032907]
  66. Miners JS, Baig S, Palmer J, Palmer LE, Kehoe PG, Love S. Ab-Degrading Enzymes in Alzheimer's Disease. *Brain Pathology.* 2008; 18:240–252. [PubMed: 18363935]
  67. Ledesma MD, Da Silva JS, Crassaerts K, Delacourte A, De Strooper B, Dotti CG. Brain plasmin enhances APP alpha-cleavage and A $\beta$  degradation and is reduced in Alzheimer's disease brains. *EMBO Rep.* 2000; 1:530–535. [PubMed: 11263499]



68. Jang H, Arce FT, Ramachandran S, Capone R, Azimova R, Kagan BL, Nussinov R, Lal R. Truncated beta-amyloid peptide channels provide an alternative mechanism for Alzheimer's Disease and Down syndrome. *Proc Natl Acad Sci U S A*. Apr 6; 2010 107(14):6538–43. DOI: 10.1073/pnas.0914251107 [PubMed: 20308552]
69. Schmaier AH. Alzheimer disease is in part a thrombohemorrhagic disorder. *J Thromb Haemost*. May; 2016 14(5):991–4. Epub 2016 Mar 16. DOI: 10.1111/jth.13277 [PubMed: 26817920]
70. Zamolodchikov D, Renné T, Strickland S. The Alzheimer's disease peptide  $\beta$ -amyloid promotes thrombin generation through activation of coagulation factor XII. *J Thromb Haemost*. May; 2016 14(5):995–1007. DOI: 10.1111/jth.13209 [PubMed: 26613657]
71. Klinger MH, Jelkmann W. Review Role of blood platelets in infection and inflammation. *J Interferon Cytokine Res*. Sep; 2002 22(9):913–22. [PubMed: 12396713]
72. Yeaman MR. Platelets in defense against bacterial pathogens. *Cell Mol Life Sci*. Feb; 2010 67(4): 525–544. [PubMed: 20013024]

### Highlights

- Additional source of  $\beta$ -amyloid in the brain
- Activated platelets are responsible for the  $A\beta$  in blood clots
- Blood thrombi contain  $\beta$ -amyloid peptide

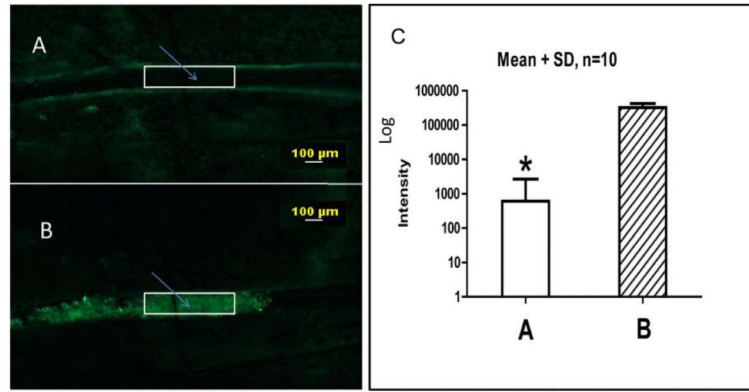


**Figure 1.** Platelet fluorescence in a blood vessel before (A) and after (B) clot formation. Fluorescence integrated density (FID) measurements were performed in the lumen in the area marked by the white box. Fluorescent platelets in the area are indicated with an arrow. A bar graph (C) summarizes mean fluorescence intensity in similar areas before and after clot formation in blood vessels in 10 different experiments. The fluorescence intensity scale is logarithmic.

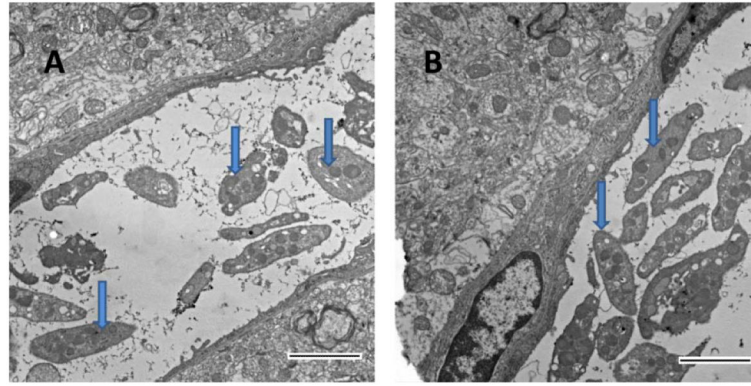


**Figure 2.** Electron photomicrography of blood clots in mouse brains. A. Platelets (arrows) were mainly present in clots in small-diameter blood vessels ( $< 6 \mu\text{m}$ ) after local clot formation. B. Platelets were also present in clots and accumulated near the endothelial wall in larger vessels ( $> 50 \mu\text{m}$ ). Fibrin fibrils are visible in the clot. Scale bars,  $2 \mu\text{m}$ .

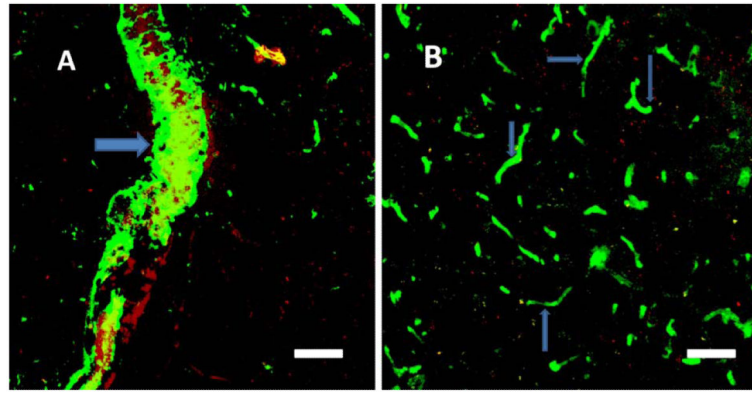


**Figure 3.**

Immunostaining of A $\beta$  peptide after clot formation in blood vessels of the V2 cortex. In the visual cortex, (A) in the large vessel (> 50  $\mu$ m, arrow) and (B) in small vessels (< 6  $\mu$ m, arrows) A $\beta$  peptide immunofluorescence was mainly concentrated in the vessel lumen. Erythrocyte-adsorbing red dye (Rose Bengal) was used for photothrombosis; thus, erythrocytes in the clots became visible in larger vessels. Scale bars, 40  $\mu$ m.

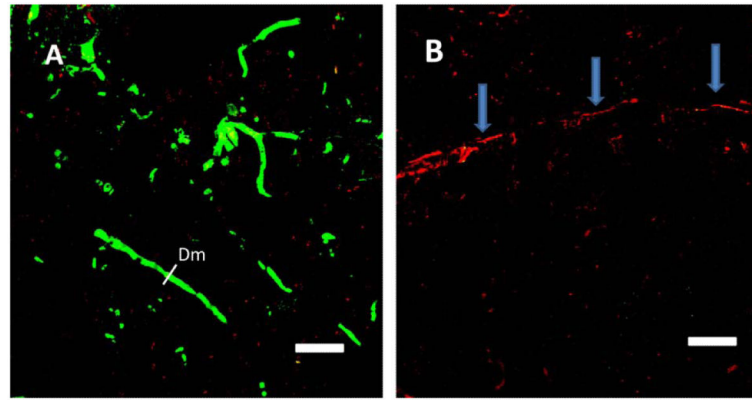


**Figure 4.** Immunostaining of A $\beta$  peptide after clot formation in blood vessels of the V2 cortex in control animals with a normal density of platelets and in thrombocytopenic mice. A. A $\beta$  immunofluorescence in blood vessels in control animals after clot formation. B. A $\beta$  immunofluorescence was practically nonexistent in thrombocytopenic animals after photothrombosis. Blood vessels in thrombocytopenic animals were recognized by an accumulation of red stain (Rose Bengal) inside the vessels (arrows). Scale bars, 40  $\mu$ m.



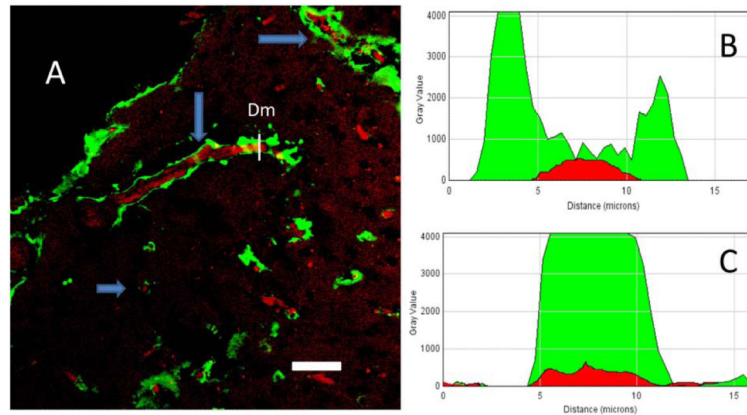


**Figure 5.**

A. Immunostaining of A $\beta$  peptides after clot formation in blood vessels of the entorhinal cortex in control mice. A $\beta$  peptide immunofluorescence is present not only in the blood vessel lumen but is also spread out from the vessels (arrows), which can be seen on longitudinally and transversely cut vessels (arrows). B. Profile plot of the diameter (Dm) of the blood vessel from Fig. 5A (entorhinal cortex). C. Profile plot of the diameter (Dm) of the blood vessel in Fig. 4A (visual cortex). Scale bar in A, 40  $\mu$ m.